THE JOURNAL OF PHYSICAL CHEMISTRY LETTERS
A JOURNAL OF THE AMERICAN CHEMICAL SOCIETY

pubs.acs.org/JPCL

Letter

# Real-Time Dynamics and Detailed Balance in Ring Polymer Surface Hopping: The Impact of Frustrated Hops

Dil K. Limbu and Farnaz A. Shakib*

Cite This: *J. Phys. Chem. Lett.* 2023, 14, 8658−8666

Read Online

ACCESS | Metrics & More | Article Recommendations | Supporting Information

**ABSTRACT:** Ring polymer surface hopping (RPSH) has been recently introduced as a well-tailored method for incorporating nuclear quantum effects, such as zero-point energy and tunneling, into nonadiabatic molecular dynamics simulations. The practical widespread usage of RPSH demands a comprehensive benchmarking of different reaction regimes and conditions with equal emphasis on demonstrating both the cons and the pros of the method. Here, we investigate the fundamental questions related to the conservation of energy and detailed balance in the context of RPSH. Using Tully's avoided crossing model as well as a 2-state quantum system coupled to a classical bath undergoing Langevin dynamics, we probe the critical problem of the proper treatment of the classically forbidden transitions stemming from the surface hopping algorithm. We show that proper treatment of these frustrated hops is key to the accurate description of real-time dynamics as well as reproducing the correct quantum Boltzmann populations.

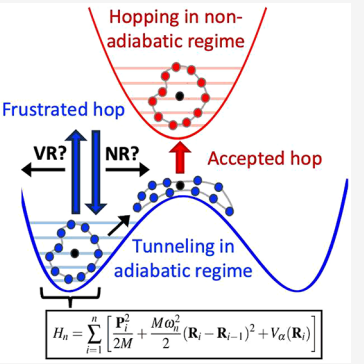




Charge transfer (CT) reactions are at the heart of energy conversion in natural and artificial (photo)-electrochemical systems. A well-known example is thermal and photoinduced (PI) proton-coupled electron transfer (PCET) reactions[1,2] which provide a more efficient pathway for natural or artificial energy conversion phenomena.[3−11] The rate and mechanism of such reactions are governed by nonadiabatic transitions between different electronic states which are widely influenced by nuclear quantum effects (NQEs) such as nuclear tunneling, vibrational relaxation, and zero-point energy (ZPE). Numerically exact methods such as hierarchical equations of motion (HEOMs)[12] and *ab initio* multiple spawning (AIMS)[13] can be used to study such reactions; however, the increasing number of degrees of freedom (DOFs) and electronic states in realistic systems impose a major limitation on the applicability of such computationally expensive methods. Mixed quantum-classical dynamics (MQCD) methodologies that allow treating the transferring electrons/protons quantum mechanically and the environmental DOFs classically have been a major breakthrough in the investigation of condensed-phase CT reactions. A distinguished example is fewest-switches surface hopping (FSSH)[14−16] which was developed in response to the need for accurate simulation of branching events ignored in the mean-field treatment of Ehrenfest[17−19] dynamics. Very soon, it became a mainstream MQCD approach for simulating nonadiabatic events owing to the ease of implementation, on top of its computational efficiency in comparison to more sophisticated but expensive methods such as the quantum-classical Liouville equation (QCLE).[20−24] Nevertheless, this trajectory-based MQCD approach, and most of its offspring methods, suffer from the lack of NQEs during the real-time dynamics simulations.

On the other hand, imaginary-time path-integral approaches, including centroid molecular dynamics (CMD)[25] and ring polymer molecular dynamics (RPMD),[26] have been successfully developed to include NQEs in molecular dynamics simulations. This inclusion of NQEs into real-time dynamics via the extended phase space of a classical ring polymer is inherently different than the semiclassical Wigner methods, i.e., the linearized semiclassical initial value representation (LSC-IVR)[27−29] and windowing methods.[30−32] While these methods show promising results for condensed-phase simulations, however, it is well-known that the combination of this quantum mechanical initial distribution with the propagation of classical trajectories, such as in FSSH, leads to zero-point energy leakage and incorrect dynamical scenarios in the long-time limit.[28,33,34] Several multistate RPMD methods[35−39] have been proposed for nonadiabatic dynamics simulations. However, they mostly suffer from the high computational cost of representing both nuclei and electrons with ring polymers limiting their applications for multielectron/multi-proton nonadiabatic dynamics.[40] In 2012, Tully and co-workers proposed a marriage between FSSH and RPMD which gave birth to ring polymer surface hopping (RPSH),[41] a

**Received:** July 27, 2023
**Accepted:** September 15, 2023
**Published:** September 21, 2023

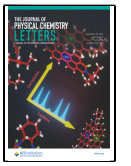





https://doi.org/10.1021/acs.jpclett.3c02085
*J. Phys. Chem. Lett.* 2023, 14, 8658−8666

promising methodology for efficient incorporation of NQEs into nonadiabatic dynamics. Since only nuclear DOFs are quantized by ring polymers, while electronic states are represented via FSSH ansatz, RPSH is a well-tailored method for investigating multielectron/multiproton transfer dynamics in condensed phases. Furthermore, electronic coherence effects are included via FSSH. This is important since the regular formulation of RPMD suffers from the lack of the effects of real-time electronic coherence.[42,43] In 2017, we established the critical roles of ZPE and nuclear tunneling, especially at low-temperature limits, by applying RPSH to model potential energy surfaces.[44] More recently, Miller and co-workers successfully employed RPSH in calculating the rate constant of scattering problems within their isomorphic Hamiltonian framework.[45] Such studies put RPSH on an upward trajectory to become a mainstream methodology for nonadiabatic molecular dynamics simulations in condensed phases subject to NQEs. For such a goal to be fulfilled, here we investigate the strengths and weaknesses of RPSH stemming from its constituent methods. We address the critical issues related to frustrated hops and how different treatments affect dynamic scenarios and the detailed balance.

We present a brief introduction to the RPSH ansatz with centroid approximation; the interested reader is referred to refs 41 and 44 for further details. In RPSH, every nuclear DOF is represented by a ring polymer, which is comprised of $n$ copies of the nuclear DOF, known as beads, connected by harmonic forces. The corresponding extended Hamiltonian is described with the following expression.

$$H_n = \sum_{i=1}^{n}\left[\frac{\mathbf{P}_i^2}{2M} + \frac{M\omega_n^2}{2}(\mathbf{R}_i - \mathbf{R}_{i-1})^2 + V_\alpha(\mathbf{R}_i)\right] \tag{1}$$

Here, $n$ is the total number of beads, and $\omega_n = n/\beta\hbar$, where $\beta = 1/k_B T$ is the reciprocal temperature. $\mathbf{P}_i$ and $\mathbf{R}_i$ represent the momentum and position of each bead of the ring polymer which moves on a single adiabatic surface $|\alpha;\mathbf{R}_i\rangle$ corresponding to the potential energy $V_\alpha(\mathbf{R}_i) = \langle\alpha;\mathbf{R}_i|\hat{V}|\alpha;\mathbf{R}_i\rangle$. At every time step of the nuclear dynamics, the position and momentum of the centroid of the ring polymer are updated as follows.

$$\bar{\mathbf{R}} = \frac{1}{n}\sum_{i=1}^{n}\mathbf{R}_i \qquad \bar{\mathbf{P}} = \frac{1}{n}\sum_{i=1}^{n}\mathbf{P}_i \tag{2}$$

At this point, according to the surface hopping algorithm, the time-dependent Schrödinger equation is numerically integrated as

$$i\hbar\dot{c}_\alpha(t) = V_\alpha(\bar{\mathbf{R}})c_\alpha(t) - i\hbar\sum_\beta \dot{\bar{\mathbf{R}}}\cdot\mathbf{d}_{\alpha\beta}(\bar{\mathbf{R}})c_\beta(t) \tag{3}$$

to confer the electronic coefficients $c_\alpha$ associated with each adiabatic surface. The important difference from the original FSSH is that this integration is carried out along the motion of the centroid. Both the energy of the adiabatic surfaces, $V_\alpha(\bar{\mathbf{R}})$, and the nonadiabatic coupling vector between surfaces, $\mathbf{d}_{\alpha\beta}(\bar{\mathbf{R}}) = \langle\alpha;\bar{\mathbf{R}}|\nabla_{\bar{\mathbf{R}}}|\beta;\bar{\mathbf{R}}\rangle$, are evaluated at the centroid level. The same goes for the probability of transition, i.e., switching between surfaces at each time step $\Delta t$, which is defined based on density matrix elements, $\rho_{\alpha\beta} = c_\alpha c_\beta^*$, as follows.

$$g_{\alpha\beta} = \frac{-2\mathrm{Re}(\rho_{\beta\alpha}^*\dot{\bar{\mathbf{R}}}\cdot\mathbf{d}_{\beta\alpha}(\bar{\mathbf{R}}))\Delta t}{\rho_{\alpha\alpha}} \tag{4}$$

The nonadiabatic transition from the current surface $\alpha$ to the next surface $\beta$ occurs if $g_{\alpha\beta}$ is greater than a randomly generated number between 0 and 1. If a transition occurs, the entire ring polymer hops to the next adiabatic surface while the velocity of each bead is rescaled along the direction of the centroid nonadiabatic coupling vector $\mathbf{d}_{\alpha\beta}(\bar{\mathbf{R}})$. Introducing $\dot{\mathbf{R}}_i'$ as the velocity of each bead after a hop, it will be calculated as follows.

$$\dot{\mathbf{R}}_i' = \dot{\mathbf{R}}_i - \lambda_{\alpha\beta}\mathbf{d}_{\alpha\beta}(\bar{\mathbf{R}})/M\cdot \tag{5}$$

Here, $\lambda_{\alpha\beta}$ is the scaling constant calculated from the following expression[16]

$$\lambda_{\alpha\beta} = \frac{1}{a_{\alpha\beta}}[b_{\alpha\beta} \pm \sqrt{b_{\alpha\beta}^2 + 2a_{\alpha\beta}c_{\alpha\beta}}] \tag{6}$$

where $a_{\alpha\beta} = \mathbf{d}_{\alpha\beta}^2(\bar{\mathbf{R}})/M$, $b_{\alpha\beta} = \dot{\bar{\mathbf{R}}}\cdot\mathbf{d}_{\alpha\beta}(\bar{\mathbf{R}})$, and $c_{\alpha\beta} = V_\alpha(\bar{\mathbf{R}}) - V_\beta(\bar{\mathbf{R}})$. While the results in this paper are obtained from rescaling velocities at the centroid level, alternatively, one can conserve the energy for the entire ring polymer. It is already shown that both methods produce qualitatively similar results.[44]

The original RPMD, by construction, yields real-time molecular dynamics (MD) trajectories that preserve exact quantum Boltzmann distribution.[26] On the other hand, not all multistate RPMD methods developed until now reproduce the expected Boltzmann populations, in part due to zero-point energy leakage.[46] RPSH is different from other multistate RPMD methods in the sense that partitioning of trajectories on different electronic states is mainly dictated by the surface hopping algorithm, albeit with respect to the position and momentum of the ring polymer centroid. It is already shown that FSSH does not exactly reproduce the Boltzmann populations but does so *approximately*,[47] a behavior that is expected from RPSH as well. Nevertheless, it is shown that the deviation of FSSH populations from Boltzmann becomes smaller and finally vanishes in two reaction regimes of small adiabatic splittings and large nonadiabatic couplings.[47] This sets surface hopping methods apart from mean-field approaches, which considerably violate detailed balance. Recently, Prezhdo and co-workers argued that proper treatment of *frustrated hops* can drastically improve detailed balance in FSSH.[48] Frustrated hops are classically forbidden transitions, the direct result of conservation of total quantum energy plus classical energy. The hopping trajectories should have enough nuclear kinetic energy to compensate for the potential energy difference between adiabatic surfaces or states. Transition attempts that do not fulfill this requirement are deemed as frustrated hops and return to their original states.[15] This leads to disruption of internal consistency despite the original promise of the surface hopping algorithm; i.e., the fraction of trajectories ending up on each state is not consistent with the average quantum probabilities anymore. Note that transitions from higher-energy to lower-energy states are always permitted, and it is the reverse that encounters rejection. As such, frustrated hops are at the core of surface hopping methods, and they have to be properly treated to (1) reach an acceptable conservation of Boltzmann populations and (2) carry out accurate electronic dynamics simulations. Tully demonstrated frustrated hops as trajectories hitting a wall and coming back, and hence the component of their velocity in the direction of the nonadiabatic coupling vector needed to be reversed.[15,16] Later, Müller and Stock showed that *not*



https://doi.org/10.1021/acs.jpclett.3c02085
J. Phys. Chem. Lett. 2023, 14, 8658−8666

reversing the velocity of frustrated hops leads to significantly improved results in photoinduced relaxation dynamics in comparison to reversing the velocity[49] hinting that the choice of treatment can be system-dependent.

Due to the importance of this issue in surface hopping method development, we follow the suite and provide a clear picture of preserving Boltzmann distributions in the RPSH framework subject to different treatments of frustrated hops. We present the results of RPSH simulations of a two-state system, with energies $\epsilon_2 > \epsilon_1$, in thermal equilibrium with a many-body classical environment. This model was employed in earlier studies of this kind with the FSSH method[48,50,51] and is well-suited for investigating thermal equilibrium. The quantum subsystem is coupled to a chain of $N$ nuclear DOFs via the first particle in the chain. The nearest-neighbor potential energy between the particles is a quartic Morse potential as

$$V(\mathbf{R}) = \sum_{i=1}^{N} V_{\mathrm{M}}(R_i - R_{i+1}) \tag{7}$$

where

$$V_{\mathrm{M}}(R) = V_0(a^2R^2 - a^3R^3 + 0.58a^4R^4) \tag{8}$$

The atom farthest from the quantum subsystem ($R_{\mathrm{N}}$) is connected to Langevin dynamics. All the particles in the chain are represented by ring polymers composed of four beads based on the convergence of the long-time adiabatic population; see the Supporting Information Figure S1. To couple the last ring polymer to Langevin dynamics we followed the well-established procedure in developing thermostated path integral formalisms where the Langevin dynamics is connected to the normal modes of ring polymers ($k$) instead of the positions of the beads.[52,53] Accordingly, the corresponding equation of motion (EOM) for the last ring polymer is written as

$$\dot{P}_{\mathrm{N}}^{(k)} = -\frac{\partial V}{\partial R_{\mathrm{N}}^{(k)}} - \gamma^{(k)}P_{\mathrm{N}}^{(k)} + \sqrt{\frac{2M\gamma^{(k)}}{\beta_{\mathrm{n}}}}\,\xi^{(k)}(t) \tag{9}$$

where $\beta_{\mathrm{n}} = \beta/n$ and $\xi^{(k)}(t)$ is an uncorrelated normal random force with unit variance and zero mean ($\langle\xi^{(k)}\rangle = 0$ and $\langle\xi^{(k)}(0)\xi^{(k)}(t)\rangle = \delta(t)$). The second term includes Langevin friction constant $\gamma^{(k)}$. For the excited modes of the ring polymer ($k > 0$) $\gamma^{(k)} = 2\omega_{\mathrm{k}}$ where $\omega_{\mathrm{k}} = 2\sin(2\pi/n)/\beta_{\mathrm{n}}\hbar$ and for the centroid mode $\gamma^{(0)} = \gamma$. All parameters of our 2-state chain model are listed in Table 1 with some variations compared to the original model.[50] Specifically, we changed the energy gap to 8.0 kJ/mol and the nonadiabatic coupling vector to $-6.0$ Å$^{-1}$ to expand our dynamics simulations to a wider range of temperatures at 200−2500 K, with a special emphasis on the low-temperature region.

**Table 1. Simulation Parameters Used for the *N*-Particle Chain Model**

| Parameter | Value | Unit |
|---|---|---|
| $N$ | 20 | |
| $m$ | 12.0 | amu |
| $V_0$ | 175.0 | kJ/mol |
| $a$ | 4.0 | Å$^{-1}$ |
| $\gamma$ | $10^{14}$ | $s^{-1}$ |
| $\Delta = \epsilon_2 - \epsilon_1$ | 8.0 | kJ/mol |
| $d_{12}$ | −6.0 | Å$^{-1}$ |

Figure 1a,b shows the RPSH populations of the two states ($P_1$ and $P_2$) over this wide range of temperatures obtained

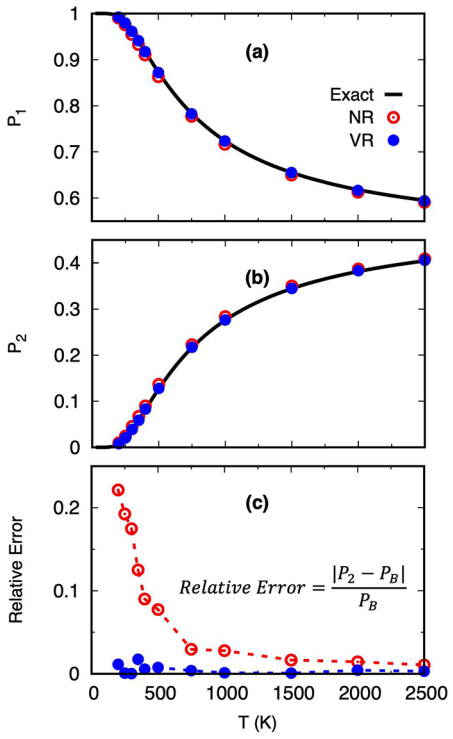


**Figure 1.** Equilibrium populations on the first state $P_1$ (a) and on the second state $P_2$ (b) of the 2-state quantum subsystem in the chain model obtained from the RPSH method with NR (⊙) and VR (•) schemes. Exact Boltzmann populations are shown as solid lines. Panel (c) shows the relative errors of NR and VR schemes in producing $P_2$ with respect to the Boltzmann population.

from the two schemes of reversing (VR) and not reversing (NR) the velocities of frustrated hops with the solid line representing the exact Boltzmann populations ($P_{\mathrm{B}}$). The RPSH populations are obtained from 1000 trajectories for 50 ps with $\Delta t = 0.01$ fs and taking the average of the last 20 ps to avoid any dependence on the initial conditions. First of all, it is very encouraging to see how RPSH, as a multistate RPMD method, is successful in closely reproducing quantum Boltzmann populations. For a better comparison between the two velocity rescaling schemes, Figure 1c demonstrates the relative error of the RPSH results for the second state stringently defined as $(P_2 - P_{\mathrm{B}})/P_{\mathrm{B}}$. As can be seen, the VR scheme shows a much smaller deviation from Boltzmann than the NR scheme, especially in the low-temperature regime.

To understand this observation, we note that generally the equilibrium populations are given by averaging the ratio of the upward and downward transition rates, $R_{\alpha\beta}$ and $R_{\beta\alpha}$, respectively, over a proper distribution function.

$$\frac{P_\beta}{P_\alpha} = \frac{\langle R_{\alpha\beta}(E_\alpha)\rangle}{\langle R_{\beta\alpha}(E_\beta)\rangle} \tag{10}$$

Here, $E_{\alpha(\beta)}$ is the nuclear kinetic energy. The analytical derivation of transition rates based on the probability of nonadiabatic transition, i.e., eq 4 in the RPSH case, and enforcing a Maxwellian distribution for the classical momenta


https://doi.org/10.1021/acs.jpclett.3c02085
J. Phys. Chem. Lett. 2023, 14, 8658−8666

is well-documented.[47,50] Conservation of the total quantum plus classical energy before and after a hop dictates that $E_\alpha + \epsilon_\alpha = E_\beta + \epsilon_\beta$. It follows that $E_\alpha - E_\beta = \epsilon_\beta - \epsilon_\alpha = \Delta$, i.e., the energy gap between quantum states. On paper, this would lead to detailed balance; however, in practice, it turns out not to be the case. For the case of FSSH, it was shown that detailed balance was not exactly preserved because (1) the ratio of attempted upward and downward transitions ($k_{\alpha\beta}/k_{\beta\alpha}$) was not unity but greater than 1, and (2) the fraction of accepted upward hops ($\chi_{\alpha\beta}$) was not equal to Boltzmann factor $\exp(-\beta\Delta)$.[47] We investigate these two features for the case of RPSH with different treatments of frustrated hops. Figure 2 shows the

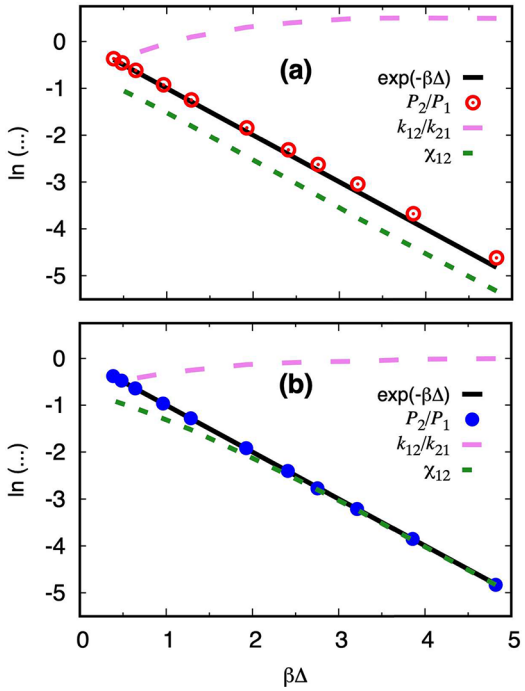


**Figure 2.** Equilibrium ratio of populations $P_2/P_1$, the ratio of the attempted upward and downward transitions $k_{12}/k_{21}$, the fraction of accepted upward hops $\chi_{12}$, and the Boltzmann factor $\exp(-\beta\Delta)$ are plotted vs the function of reduced temperature $\beta\Delta$ for NR (⊙) (a) and VR (●) (b) schemes. The $y$-axis is presented on the logarithmic scale.

equilibrium ratio of populations, $P_2/P_1$, as well as $k_{12}/k_{21}$ and $\chi_{12}$ for the chain model studied here for the NR and VR schemes. As can be seen, the reason behind the better treatment of detailed balance in the VR scheme compared to the NR scheme is that not only $k_{12}/k_{21}$ reaches unity but also $\chi_{12}$ follows the Boltzmann factor more closely. This confirms Tully's original proposal in assuming frustrated hops hitting a wall and coming back, which necessitates their velocity to be reversed.

Before concluding this section, we comment on the effect of Langevin friction on RPSH simulations with the VR scheme. As was noted before, damping of the free ring polymer internal modes is not a certain prescription for the accurate calculation of dynamical properties.[53] Hence, we introduce a damping parameter $\lambda$ which acts on the Langevin friction to allow us to explore overdamping, i.e., $\lambda > 1$, and under-damping, i.e., $\lambda < 1$. Figure 3 demonstrates the relative error in producing $P_2$ using different damping parameters. Clearly overdamping has the highest error in producing correct $P_2$ though the difference

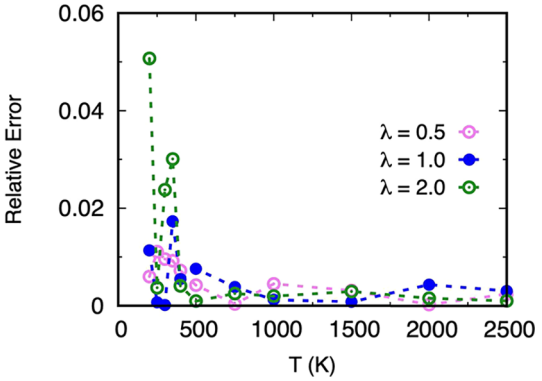


**Figure 3.** Relative errors of VR schemes in producing $P_2$ with respect to the Boltzmann population with different damping parameters $\lambda$. Note that $\lambda = 1$ corresponds to the RPSH results with the VR scheme reported in Figure 1.

between the three sets of results does not exceed ~4%, which is rather negligible. Nevertheless, one should pay attention that in this model, Langevin dynamics is only coupled to the last DOF of a chain of 20 particles. The damping effect can be more pronounced in systems with more complicated environments and should therefore be investigated before the generalization of results.

Overall, with the RPSH simulation of the chain model, we confirm the findings of Prezhdo and co-workers on FSSH[48] that reversing velocity induces a quantum back reaction which imparts a more Maxwellian behavior to the classical coordinates. Recently, the effect of different treatments of frustrated hops in preserving detailed balance was also studied in the case of fragmented orbital-based surface hopping (FOB-SH) in the context of electron−hole transfer in a dimer of an ethylene-like molecule.[54] Similar to the earlier works,[47,48] as well as the results presented here, it was suggested that the VR scheme has an improving effect on preserving detailed balance. Nevertheless, we recommend caution in applying such conclusions to RPSH since it is the combination of two different ansatz. The question remains whether the VR scheme has an adverse effect on the dynamics and whether these two algorithms, RPMD and FSSH, would cooperate or collide. Hence, we expand this study to simulate the electronic dynamics in models in which the electronic states and their coupling are affected by the motion of nuclear DOFs.

Here, we focus on Tully's single avoided crossing (SAC) model and establish the effect of reversing or not reversing the velocity of frustrated hops on the adiabatic population transfer profile in the low to medium momentum regions where the NQEs are paramount. For this model, we also employ two different remedies suggested by Truhlar[55] and Subotnik[56] for treating frustrated hops. Jasper and Truhlar combined the features of reversing and not reversing the velocity in a prescription called $\Delta V$ which, whenever a frustrated hop occurs, allows the trajectory to feel the target adiabatic state $\beta$. Accordingly, in the case of a frustrated hop in RPSH, we compare $\bar{\mathbf{R}} \cdot \mathbf{d}_{\alpha\beta}$ to the component of the force in the direction of the centroid nonadiabatic coupling vector, defined as follows.

$$F_\beta = -\nabla V_\beta(\bar{\mathbf{R}}) \cdot \mathbf{d}_{\alpha\beta}(\bar{\mathbf{R}}) \tag{11}$$

If these two quantities have the same sign, we do not reverse the velocity but will do so if they have opposite signs. On the



https://doi.org/10.1021/acs.jpclett.3c02085
J. Phys. Chem. Lett. 2023, 14, 8658−8666

other hand, Jain and Subotnik suggested a comparison between the components of forces from both the current and the target adiabatic states. Accordingly, in RPSH, we calculate

$$(\mathbf{d}_{\alpha\beta}(\bar{\mathbf{R}})\cdot(-\nabla V_{\alpha}(\bar{\mathbf{R}})))(\mathbf{d}_{\alpha\beta}(\bar{\mathbf{R}})\cdot(-\nabla V_{\beta}(\bar{\mathbf{R}}))) \quad (12)$$

and reverse the velocity if it is smaller than zero. Henceforth, we shall call this approach $\Delta V^2$ as it bears a resemblance to the $\Delta V$ approach. Both these approaches are more refined than the phenomenological VR scheme in their criteria for reversing the velocity of frustrated hops and were shown to improve the quality of FSSH results. Hence, it is interesting to investigate their effect in the case of RPSH or any other surface hopping algorithm.

The SAC model is defined by a 2 × 2 diabatic matrix with the details being provided in Supporting Information. Diagonalizing this matrix yields two adiabatic states with a single avoided crossing, shown in the inset of Figure 4a, and a corresponding nonadiabatic coupling vector, shown in orange. This 2-state system is then coupled to one nuclear DOF whose wave function is initialized on state $|1\rangle$ as a Gaussian wavepacket in the following form.

$$G(R) = \left(\frac{2\alpha}{\pi}\right)^{1/4} \exp(-\alpha(R - R_0)^2 + ik(R - R_0)) \quad (13)$$

This is manifested in a Gaussian distribution of nuclear position around $R_0 = -15$ au with the width of $\sigma_R = 1/\sqrt{2\alpha}$. Here, $\alpha = 0.25$ au and $k$ is the deterministic incoming momentum of the nuclear DOF with the mass $M = 2000$ au. For RPSH simulations, the classical DOF is expanded to a ring polymer with four beads whose initial positions are randomly selected from the Gaussian distribution. The choice of four beads for the ring polymer is based on the convergence of the adiabatic populations.[44] Dynamics simulations under microcanonical conditions are carried out using a fictitious temperature that matches the initial kinetic energy of this 1-dimensional system through $E = \frac{1}{2}k_B T$. Though this is an *ad hoc* choice, generally, temperature can be used as an indirect measure of the energy of systems. Furthermore, it was shown that other classes of multistate RPMD methods produce reliable real-time photoexcited dynamics based on similar assumptions.[37,57]

We first focus on the branching probabilities as a function of the incoming momentum obtained from an ensemble of 10,000 RPSH trajectories run for 0.5 ps with a time-step of 1 au (~0.024 fs). Branching probabilities show the final adiabatic populations of states $|1\rangle$ and $|2\rangle$ with differentiating between trajectories that upon reaching the avoided crossing transmit from the reactant to the product side or reflect back to the reactant side. Figure 4 demonstrates the branching probabilities, namely, transmission and reflection on state $|1\rangle$ ($T_1$ and $R_1$, respectively), and transmission on state $|2\rangle$ ($T_2$) in the low- to intermediate-momentum regions divided by a vertical line. According to the exact results shown in dashed lines, the incoming momentum in the low-momentum region, i.e., $k$ = 2−6.5 a.u, is not sufficient for nonadiabatic transitions to happen, and the wavepacket moves adiabatically on state $|1\rangle$. This dynamics is governed by nuclear tunneling where exact results show a smooth increase of $T_1$ at the expense of a decrease in $R_1$. We have previously shown[44] that FSSH fails to capture this quantum-mechanical phenomenon but RPSH

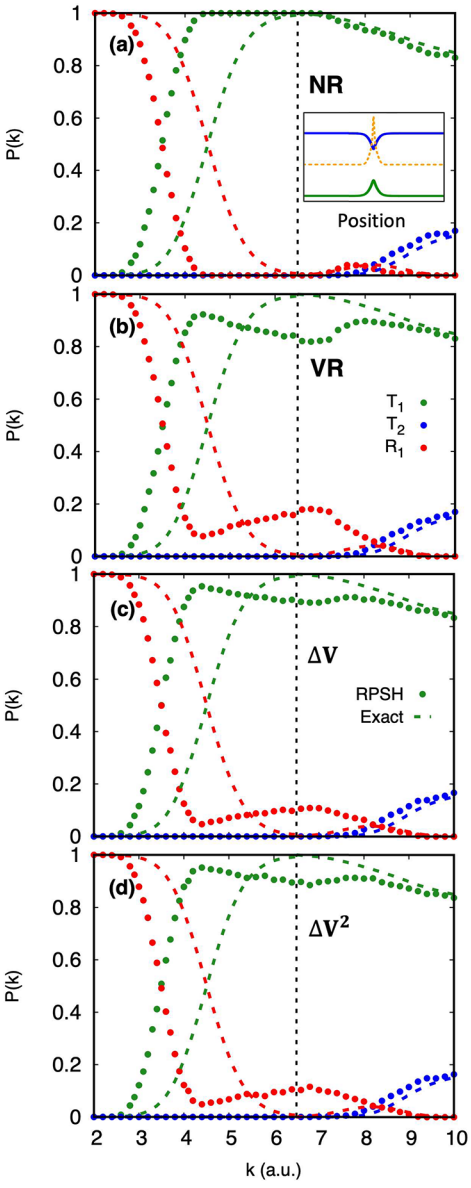


**Figure 4.** Branching probabilities in the SAC model, inset in (a), at the low and intermediate momentum regions (divided by a vertical line). Transmission and reflection on state $|1\rangle$, $T_1$ and $R_1$, are shown along with transmission on state $|2\rangle$, $T_2$. Four panels demonstrate the results of RPSH simulations with four different treatments of frustrated hops vs exact results. Please see the Supporting Information, Figure S3, for a magnified plot of $R_1$ and $T_2$ in the intermediate momentum region.

recovers the correct physical behavior, i.e., a smooth transition between $R_1$ and $T_1$, through the extended phase-space of a classical ring polymer. Here, we evaluate the effects of four different treatments of frustrated hops on branching probabilities, namely, VR or NR along with $\Delta V$ and $\Delta V^2$ approaches[55,56] as explained previously. As can be seen in Figure 4, the four schemes show similar behavior in capturing the smooth transition in the very low-momentum region but start deviating around $k$ = 3.3 au where only the NR scheme follows the same behavior of the exact results in 100% reversal of $R_1$ to $T_1$. The other three schemes underestimate the magnitude of adiabatic transmission at higher values of momentum.



https://doi.org/10.1021/acs.jpclett.3c02085
J. Phys. Chem. Lett. 2023, 14, 8658−8666

To explain what causes this behavior, we note that in the *adiabatic* reaction regime, RPSH is expected to go back to RPMD with the well-established inclusion of NQEs (nuclear tunneling here) into the dynamics. However, because of the presence of the FSSH algorithm, the nuclear trajectories moving toward avoided crossing on state $|1\rangle$ experience *attempted* transitions. Since there is not enough kinetic energy to overcome the energy difference between states $|1\rangle$ and $|2\rangle$, they come back to state $|1\rangle$; i.e., they experience frustrated hops even in the *adiabatic* reaction regime. We emphasize that this is solely the result of combining the RPMD algorithm with FSSH. The trajectories facing frustrated hops in the NR scheme still continue their motion with positive momentum. They tunnel through the energy barrier on state $|1\rangle$ and end up on the product side. In other words, frustrated hops do not interrupt the motion of the adiabatic trajectories in the RPSH-NR method. On the other hand, fully or partially reversing the velocity in the other three schemes forces such a trajectory to go back to the reactant side negating the possibility of tunneling through the energy barrier. This results in an artificial increase of $R_1$ in the expense of decrease in $T_1$.

As we increase the momentum beyond $k = 6.5$ au, we reach the intermediate reaction regime, i.e., the RHS of the vertical line in Figure 4, where nonadiabatic trajectories appear alongside adiabatic trajectories. In this region, still, the majority of trajectories travel from reactant to product side *adiabatically* while a smaller fraction successfully transitions from state $|1\rangle$ to $|2\rangle$. The number of these *nonadiabatic* trajectories naturally increases with the increase of the initial momentum and results in a smooth increase of $T_2$ as shown in Figure 4 by all four schemes of RPSH. This smooth increase of $T_2$, which we have already shown is missed in FSSH,[44] is due to inclusion of zero-point energy in the upper-state dynamics within the RPSH formalism. On the other hand, there is still a significant deviation between NR and the other three schemes in retrieving the correct physical behavior in the case of $T_1$ and $R_1$ with only the former being successful. This is still related to the frustrated hops in the big fraction of adiabatic trajectories which are happening alongside the nonadiabatic ones. However, as the momentum increases, more attempted upward hops have enough kinetic energy to reach the upper state. This means a decrease in frustrated hops beyond $k = 7$ au and simultaneously the decrease of artificially high values of $R_1$ in all three velocity reversing schemes. Toward the far right end of the intermediate-momentum region, $R_1$ and $T_1$ probabilities of these three schemes better reproduce the exact results, as the NR scheme had done all the way through. It should be noted that one can enforce the correct dynamics even with total or partial velocity reversal by not allowing the trajectories to attempt a transition. However, that needs *a priori* information about the reaction regimes of different systems.

Overall, in the 2-state chain model, the VR scheme leads to more accurate preservation of detailed balance while in the SAC model the NR scheme reproduces the correct dynamical scenario. One should note the essential differences between the two models with the lack of an avoided crossing in the chain model being the most important one. The chain model is designed to represent a quantum system in thermal equilibrium with its surroundings and is not suitable for investigating scattering events. Furthermore, despite different results, we characterize a similar phenomenon in the RPSH studies of these two models. Figure 5 demonstrates the

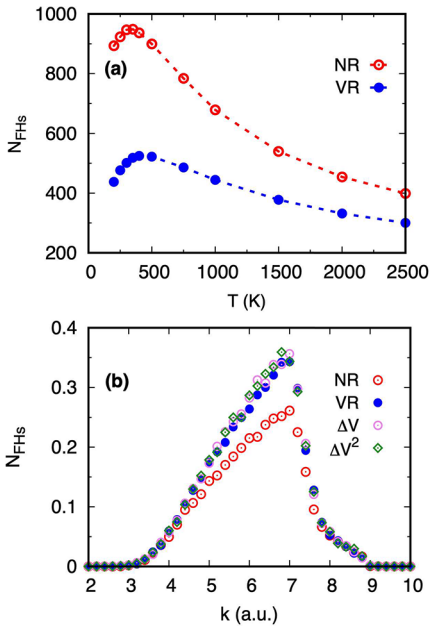


**Figure 5.** Number of frustrated hops averaged over the number of trajectories in the chain model over a range of temperatures (a) and in the SAC model over a range of initial momentum (b) obtained from RPSH methods with different velocity rescaling schemes.

number of frustrated hops by using different treatments in the two models studied here. One can recognize that in both models, regardless of their inherent differences, the scheme with the fewest number of frustrated hops leads to a better result, i.e., the VR scheme in Figure 5a and the NR scheme in Figure 5b. Hence, in comparison between the two models, we recommend here the number of frustrated hops as a useful indicator of the performance of the method. Interestingly, a more refined indicator can be recognized by focusing on the three schemes that fully or partially reverse the velocity of frustrated hops. Figure 5b shows that VR, $\Delta V$, and $\Delta V^2$ schemes have a similar number of frustrated hops. In spite of that, a closer look at panels b–d of Figure 4 reveals that the VR scheme has more deviation from the correct physical behavior than the other two schemes. This is related to the number of instances that criteria for accepting the reversal of velocity of frustrated hops are met in the $\Delta V$ and $\Delta V^2$ schemes, see the Supporting Information Figure S2. Since they have a similar number of acceptance instances, they show similar deviation from correct $R_1$ and $T_1$ while they both operate better than the VR scheme, which reverses the velocity of frustrated hops at all times. These suggestion still require further verification in other classes of systems and in investigating different properties before it can be generalized.

To summarize, we critically revisited RPSH nonadiabatic molecular dynamics methodology in order to shed light on its accuracy and validity limits. The most exciting aspect of RPSH, i.e., the inclusion of NQEs into nonadiabatic molecular dynamics, can be further harvested if the advantages and disadvantages of the method are carefully investigated and documented in different systems and reaction regimes. We employed four different schemes of velocity rescaling to treat frustrated hops in RPSH and study their effects on preserving correct quantum Boltzmann distribution as well as accurate description of quantum dynamics using two different models. For the 2-state quantum system coupled to a chain of classical


https://doi.org/10.1021/acs.jpclett.3c02085
J. Phys. Chem. Lett. 2023, 14, 8658–8666

DOFs, we showed that reversing the velocity (VR) after each frustrated hop improves detailed balance in a range of low to high temperatures. On the other hand, investigating the real-time dynamics in Tully's avoided crossing model, we found that not reversing the velocity (NR) is the only scheme that gives a proper description of the branching probabilities on the two adiabatic states. This is the result of an interplay between frustrated hops and nuclear tunneling in the adiabatic reaction regime. Overall, we advise caution against *a priori* assumptions in the choice of a treatment for frustrated hops in RPSH applications. The reason is that the method is composed of two different algorithms that may cooperate or collide in different model systems. Nevertheless, we found that in both models, the velocity rescaling scheme that gives fewer number of frustrated hops produces better results. We also present RPSH together with four remedies for treating frustrated hops in different model systems studied in this work via a parallelized user-friendly software coined the SHARP pack, short for surface hopping and ring polymer package. The pilot version of this software is available from our GitHub repository.[58] These studies/products collectively portray a clearer picture of the functionality of the path integral formalism in the inclusion of NQEs in molecular dynamics simulations, which is crucial for future developments via a unified community effort.

To further bring RPSH to the mainstream, research should be directed to (i) a systematic implementation of decoherence correction and (ii) implementing contraction schemes for large-scale simulations. Surface hopping methods take care of electronic coherence; however, they have always been plagued with the overcoherence problem or neglect of decoherence.[59] We have already shown that, in contrast to FSSH, RPSH can capture distribution-dependent decoherence in Tully's "extended coupling with reflection" model even with a deterministic initial momentum.[44] Application of RPSH in more sophisticated models designed for the investigation of decoherence as well as equipping it with different decoherence correction schemes is currently being pursued in our group. On the other hand, using a contraction scheme, long-range forces can be evaluated on a ring polymer with fewer beads than needed to evaluate the short-range forces. Such contraction schemes are already established for RPMD simulations[60] and shown to reduce the cost of dynamic simulation of liquid water considerably.[61] This computational efficiency will be of utmost importance for nonadiabatic RPSH simulations of realistic systems which are inherently more expensive than adiabatic RPMD.

## ■ ASSOCIATED CONTENT

### Data Availability Statement

The data that support the findings of this study are available within the article and its Supporting Information. The software used to produce the data is shared via our GitHub repository.

### Supporting Information

The Supporting Information is available free of charge at https://pubs.acs.org/doi/10.1021/acs.jpclett.3c02085.

The details of the SAC model, convergence tests with respect to the number of beads, instances of velocity reversal in the VR, $\Delta V$, and $\Delta V^2$ schemes, and a magnified plot of population transfer dynamics of the SAC model in the intermediate momentum region (PDF)

## ■ AUTHOR INFORMATION


### Corresponding Author

**Farnaz A. Shakib** − *Department of Chemistry and Environmental Science, New Jersey Institute of Technology, Newark, New Jersey 07102, United States;* orcid.org/0000-0003-1432-2812; Email: shakib@njit.edu

### Author

**Dil K. Limbu** − *Department of Chemistry and Environmental Science, New Jersey Institute of Technology, Newark, New Jersey 07102, United States;* orcid.org/0000-0001-9196-9498

Complete contact information is available at: https://pubs.acs.org/10.1021/acs.jpclett.3c02085


### Notes

The authors declare no competing financial interest.

## ■ ACKNOWLEDGMENTS

The authors acknowledge support from the New Jersey Institute of Technology (NJIT). This research has been enabled by the use of computing resources and technical support provided by the HPC center at NJIT. This work partially used Bridges2 at Pittsburgh Supercomputing Center through allocation CHE200007 from the Extreme Science and Engineering Discovery Environment (XSEDE), which was supported by National Science Foundation Grant No. 1548562.[62]

## ■ REFERENCES


(1) Huynh, M. H. V.; Meyer, T. J. Proton-Coupled Electron Transfer. *Chem. Rev.* **2007**, *107*, 5004−5064.

(2) Hammes-Schiffer, S.; Stuchebrukhov, A. A. Theory of Coupled Electron and Proton Transfer Reactions. *Chem. Rev.* **2010**, *110*, 6939−6960.

(3) Diner, B. A.; Rappaport, F. Structure, Dynamics, and Energetics of the Primary Photochemistry of Photosystem II of Oxygenic Photosynthesis. *Annu. Rev. Plant Biol.* **2002**, *53*, 551−580.

(4) Babcock, G. T.; Wikström, M. Oxygen Activation and the Conservation of Energy in Cell Respiration. *Nature* **1992**, *356*, 301−309.

(5) Bediako, D. K.; Solis, B. H.; Dogutan, D. K.; Roubelakis, M. M.; Maher, A. G.; Lee, C. H.; Chambers, M. B.; Hammes-Schiffer, S.; Nocera, D. G. Role of Pendant Proton Relays and Proton-Coupled Electron Transfer on the Hydrogen Evolution Reaction by Nickel Hangman Porphyrins. *Proc. Natl. Acad. Sci. U. S. A.* **2014**, *111*, 15001−15006.

(6) Dempsey, J. L. Proton-Coupled Electron Transfer: Metal Hydrides Find the Sweet Spot. *Nat. Chem.* **2015**, *7*, 101−102.

(7) Liu, T.; Guo, M.; Orthaber, A.; Lomoth, R.; Lundberg, M.; Ott, S.; Hammarström, L. Accelerating Proton-Coupled Electron Transfer of Metal Hydrides in Catalyst Model Reactions. *Nat. Chem.* **2018**, *10*, 881−887.

(8) Kurtz, D. A.; Dempsey, J. L. Proton-Coupled Electron Transfer Kinetics for the Photoinduced Generation of a Cobalt(III)-Hydride Complex. *Inorg. Chem.* **2019**, *58*, 16510−16517.

(9) Boschloo, G.; Hagfeldt, A. Spectroelectrochemistry of Nanostructured NiO. *J. Phys. Chem. B* **2001**, *105*, 3039−3044.

(10) Taggart, A. D.; Evans, J. M.; Li, L.; Lee, K. J.; Dempsey, J. L.; Kanai, Y.; Cahoon, J. F. Enabling Aqueous NiO Photocathodes by Passivating Surface Sites That Facilitate Proton-Coupled Charge Transfer. *ACS Appl. Energy Mater.* **2020**, *3*, 10702−10713.

(11) Li, Y.; Hui, D.; Sun, Y.; Wang, Y.; Wu, Z.; Wang, C.; Zhao, J. Boosting Thermo-Photocatalytic $CO_2$ Conversion Activity by Using Photosynthesis-Inspired Electron-Proton-Transfer Mediators. *Nat. Commun.* **2021**, *12*, 123.

(12) Song, K.; Shi, Q. Theoretical Study of Photoinduced Proton Coupled Electron Transfer Reaction Using the Non-Perturbative Hierarchical Equations of Motion Method. *J. Chem. Phys.* **2017**, *146*, 184108.
(13) Pijeau, S.; Foster, D.; Hohenstein, E. G. Excited-State Dynamics of a Benzotriazole Photostabilizer: 2-(2'-Hydroxy-5' Methylphenyl)Benzotriazole. *J. Phys. Chem. A* **2017**, *121*, 6377−6387.
(14) Tully, J. C.; Preston, R. K. Trajectory Surface Hopping Approach to Nonadiabatic Molecular Collisions: The Reaction of $H^+$ with $D_2$. *J. Chem. Phys.* **1971**, *55*, 562−572.
(15) Tully, J. C. Molecular Dynamics with Electronic Transitions. *J. Chem. Phys.* **1990**, *93*, 1061−1071.
(16) Hammes-Schiffer, S.; Tully, J. C. Proton Transfer in Solution: Molecular Dynamics with Quantum Transitions. *J. Chem. Phys.* **1994**, *101*, 4657−4667.
(17) Ehrenfest, P. Bemerkung über die angenäherte gältigkeit der klassischen mechanik innerhalb der quantenmechanik. *Eur. Phys. J. A* **1927**, *45*, 455−457.
(18) Mittleman, M. H. Theory of Relativistic Effects on Atoms: Configuration-Space Hamiltonian. *Phys. Rev. A* **1981**, *24*, 1167−1175.
(19) Sawada, S.-I.; Nitzan, A.; Metiu, H. Mean-Trajectory Approximation for Charge- and Energy-Transfer Processes at Surfaces. *Phys. Rev. B* **1985**, *32*, 851−867.
(20) Kapral, R.; Ciccotti, G. Mixed Quantum-Classical Dynamics. *J. Chem. Phys.* **1999**, *110*, 8919−8929.
(21) Nielsen, S.; Kapral, R.; Ciccotti, G. Non-Adiabatic Dynamics in Mixed Quantum-Classical Systems. *J. Stat. Phys.* **2000**, *101*, 225−242.
(22) Hanna, G.; Kapral, R. Quantum-Classical Liouville Dynamics of Nonadiabatic Proton Transfer. *J. Chem. Phys.* **2005**, *122*, 244505.
(23) Shakib, F.; Hanna, G. Mixed Quantum-Classical Liouville Approach for Calculating Proton-Coupled Electron-Transfer Rate Constants. *J. Chem. Theory Comput.* **2016**, *12*, 3020−3029.
(24) Shakib, F. A.; Hanna, G. New Insights into the Nonadiabatic State Population Dynamics of Model Proton-Coupled Electron Transfer Reactions from the Mixed Quantum-Classical Liouville Approach. *J. Chem. Phys.* **2016**, *144*, 024110.
(25) Cao, J.; Voth, G. A. The Formulation of Quantum Statistical Mechanics Based on the Feynman Path Centroid Density. IV. Algorithms for Centroid Molecular Dynamics. *J. Chem. Phys.* **1994**, *101*, 6168−6183.
(26) Craig, I. R.; Manolopoulos, D. E. Quantum Statistics and Classical Mechanics: Real-Time Correlation Functions from Ring Polymer Molecular Dynamics. *J. Chem. Phys.* **2004**, *121*, 3368−3373.
(27) Wang, H.; Sun, X.; Miller, W. H. Semiclassical Approximations for the Calculation of Thermal Rate Constants for Chemical Reactions in Complex Molecular Systems. *J. Chem. Phys.* **1998**, *108*, 9726−9736.
(28) Sun, X.; Wang, H.; Miller, W. H. Semiclassical Theory of Electronically Nonadiabatic Dynamics: Results of a Linearized Approximation to the Initial Value Representation. *J. Chem. Phys.* **1998**, *109*, 7064−7074.
(29) Miller, W. H. Generalization of the Linearized Approximation to the Semiclassical Initial Value Representation for Reactive Flux Correlation Functions. *J. Phys. Chem. A* **1999**, *103*, 9384−9387.
(30) Cotton, S. J.; Miller, W. H. The Symmetrical Quasi-Classical Model for Electronically Non-Adiabatic Processes Applied to Energy Transfer Dynamics in Site-Exciton Models of Light-Harvesting Complexes. *J. Chem. Theory Comput.* **2016**, *12*, 983−991.
(31) Cotton, S. J.; Miller, W. H. Trajectory-Adjusted Electronic Zero Point Energy in Classical Meyer-Miller Vibronic Dynamics: Symmetrical Quasiclassical Application to Photodissociation. *J. Chem. Phys.* **2019**, *150*, 194110.
(32) Cotton, S. J.; Miller, W. H. A Symmetrical Quasi-Classical Windowing Model for the Molecular Dynamics Treatment of Non-Adiabatic Processes Involving Many Electronic States. *J. Chem. Phys.* **2019**, *150*, 104101.
(33) Guo, Y.; Thompson, D. L.; Sewell, T. D. Analysis of the Zero-Point Energy Problem in Classical Trajectory Simulations. *J. Chem. Phys.* **1996**, *104*, 576−582.
(34) Ben-Nun, M.; Levine, R. D. On the Zero Point Energy in Classical Trajectory Computations. *J. Chem. Phys.* **1996**, *105*, 8136−8141.
(35) Ananth, N. Mapping Variable Ring Polymer Molecular Dynamics: A Path-Integral Based Method for Nonadiabatic Processes. *J. Chem. Phys.* **2013**, *139*, 124102.
(36) Richardson, J. O.; Thoss, M. Communication: Nonadiabatic Ring-Polymer Molecular Dynamics. *J. Chem. Phys.* **2013**, *139*, 031102.
(37) Duke, J. R.; Ananth, N. Simulating Excited State Dynamics in Systems with Multiple Avoided Crossings Using Mapping Variable Ring Polymer Molecular Dynamics. *J. Phys. Chem. Lett.* **2015**, *6*, 4219−4223.
(38) Duke, J. R.; Ananth, N. Mean Field Ring Polymer Molecular Dynamics for Electronically Nonadiabatic Reaction Rates. *Faraday Discuss.* **2016**, *195*, 253−268.
(39) Chowdhury, S. N.; Huo, P. Coherent State Mapping Ring Polymer Molecular Dynamics for Non-Adiabatic Quantum Propagations. *J. Chem. Phys.* **2017**, *147*, 214109.
(40) Kretchmer, J. S.; Miller, T. F. Direct Simulation of Proton-Coupled Electron Transfer Across Multiple Regimes. *J. Chem. Phys.* **2013**, *138*, 134109.
(41) Shushkov, P.; Li, R.; Tully, J. C. Ring Polymer Molecular Dynamics with Surface Hopping. *J. Chem. Phys.* **2012**, *137*, 22A549.
(42) Menzeleev, A. R.; Ananth, N.; Miller, T. F. Direct Simulation of Electron Transfer Using Ring Polymer Molecular Dynamics: Comparison with Semiclassical Instanton Theory and Exact Quantum Methods. *J. Chem. Phys.* **2011**, *135*, 074106.
(43) Habershon, S.; Manolopoulos, D. E.; Markland, T. E.; Miller, T. F. Ring-Polymer Molecular Dynamics: Quantum Effects in Chemical Dynamics from Classical Trajectories in an Extended Phase Space. *Annu. Rev. Phys. Chem.* **2013**, *64*, 387−413.
(44) Shakib, F. A.; Huo, P. Ring Polymer Surface Hopping: Incorporating Nuclear Quantum Effects into Nonadiabatic Molecular Dynamics Simulations. *J. Phys. Chem. Lett.* **2017**, *8*, 3073−3080.
(45) Tao, X.; Shushkov, P.; Miller, T. F. Path-Integral Isomorphic Hamiltonian for Including Nuclear Quantum Effects in Non-Adiabatic Dynamics. *J. Chem. Phys.* **2018**, *148*, 102327.
(46) Ananth, N. Path Integrals for Nonadiabatic Dynamics: Multistate Ring Polymer Molecular Dynamics. *Annu. Rev. Phys. Chem.* **2022**, *73*, 299−322.
(47) Schmidt, J. R.; Parandekar, P. V.; Tully, J. C. Mixed Quantum-Classical Equilibrium: Surface Hopping. *J. Chem. Phys.* **2008**, *129*, 044104.
(48) Sifain, A. E.; Wang, L.; Prezhdo, O. V. Communication: Proper Treatment of Classically Forbidden Electronic Transitions Significantly Improves Detailed Balance in Surface Hopping. *J. Chem. Phys.* **2016**, *144*, 211102.
(49) Müller, U.; Stock, G. Surface-Hopping Modeling of Photoinduced Relaxation Dynamics on Coupled Potential-Energy Surfaces. *J. Chem. Phys.* **1997**, *107*, 6230−6245.
(50) Parandekar, P. V.; Tully, J. C. Mixed Quantum-Classical Equilibrium. *J. Chem. Phys.* **2005**, *122*, 094102.
(51) Parandekar, P. V.; Tully, J. C. Detailed Balance in Ehrenfest Mixed Quantum-Classical Dynamics. *J. Chem. Theory Comput.* **2006**, *2*, 229−235.
(52) Ceriotti, M.; Parrinello, M.; Markland, T. E.; Manolopoulos, D. E. Efficient Stochastic Thermostatting of Path Integral Molecular Dynamics. *J. Chem. Phys.* **2010**, *133*, 124104.
(53) Rossi, M.; Ceriotti, M.; Manolopoulos, D. E. How to Remove the Spurious Resonances from Ring Polymer Molecular Dynamics. *J. Chem. Phys.* **2014**, *140*, 234116.
(54) Spencer, J.; Gajdos, F.; Blumberger, J. FOB-SH: Fragment Orbital-Based Surface Hopping for Charge Carrier Transport in Organic and Biological Molecules and Materials. *J. Chem. Phys.* **2016**, *145*, 064102.
(55) Jasper, A. W.; Truhlar, D. G. Improved Treatment of Momentum at Classically Forbidden Electronic Transitions in Trajectory Surface Hopping Calculations. *Chem. Phys. Lett.* **2003**, *369*, 60−67.


https://doi.org/10.1021/acs.jpclett.3c02085
J. Phys. Chem. Lett. 2023, 14, 8658−8666

(56) Jain, A.; Subotnik, J. E. Surface Hopping, Transition State Theory, and Decoherence. II. Thermal Rate Constants and Detailed Balance. *J. Chem. Phys.* **2015**, *143*, 134107.
(57) Chowdhury, S. N.; Huo, P. State Dependent Ring Polymer Molecular Dynamics for Investigating Excited Nonadiabatic Dynamics. *J. Chem. Phys.* **2019**, *150*, 244102.
(58) Limbu, D. K.; Shakib, F. A. SHARP Pack: Non-Adiabatic Molecular Dynamics Simulation Software Package. Available from: https://github.com/fashakib/SHARP_pack.
(59) Subotnik, J. E.; Shenvi, N. Decoherence and Surface Hopping: When Can Averaging over Initial Conditions Help Capture the Effects of Wave Packet Separation? *J. Chem. Phys.* **2011**, *134*, 244114.
(60) Markland, T. E.; Manolopoulos, D. E. An Efficient Ring Polymer Contraction Scheme for Imaginary Time Path Integral Simulations. *J. Chem. Phys.* **2008**, *129*, 024105.
(61) Markland, T. E.; Manolopoulos, D. E. A Refined Ring Polymer Contraction Scheme for Systems with Electrostatic Interactions. *Chem. Phys. Lett.* **2008**, *464*, 256−261.
(62) Towns, J.; Cockerill, T.; Dahan, M.; Foster, I.; Gaither, K.; Grimshaw, A.; Hazlewood, V.; Lathrop, S.; Lifka, D.; Peterson, G. D.; Roskies, R.; Scott, J. R.; Wilkins-Diehr, N. XSEDE: Accelerating Scientific Discovery. *Comput. Sci. Eng.* **2014**, *16*, 62−74.



https://doi.org/10.1021/acs.jpclett.3c02085
*J. Phys. Chem. Lett.* 2023, 14, 8658−8666